

ORIGINAL ARTICLE

Cellular Uptake of *Catharanthus roseus*-Silver Nanoparticles in Human Hepatocellular Carcinoma HepG2 Cells

Nur Asna Azhar¹, Siti Aishah Abu Bakar^{1,2}, Siti Hawa Ngalim¹, Nor Hazwani Ahmad¹

¹ Department of Biomedical Science, Advanced Medical and Dental Institute, Universiti Sains Malaysia, Bertam 13200 Kepala Batas, Pulau Pinang, Malaysia.

² Faculty of Bioresources and Food Industry, Universiti Sultan Zainal Abidin, Besut Campus, 22200 Besut, Terengganu Darul Iman, Malaysia.

ABSTRACT

Introduction: Nanoparticles exhibit unique features and currently at the forefront of cutting-edge research. Silver nanoparticles (AgNPs) are among the most promising and widely commercialised nanoproducts in various fields. The interaction of these AgNPs with cells remain unclear to connect with its toxicological endpoints. The aim of this study was to investigate the cellular uptake of *C. roseus*-AgNPs in hepatocellular carcinoma cells HepG2. **Methods:** The HepG2 cells were treated with the mean IC_{50} value of *C. roseus*-AgNPs which was 4.95 ± 0.26 $\mu\text{g/mL}$ for 24, 48 and 72 hours. The effects were compared with the untreated cells and other treatments which include camptothecin, *C. roseus*-aqueous extract, and AgNO_3 . Inductively coupled plasma optical emission spectroscopy (ICP-OES) was used to quantify the intracellular Ag^+ and Ca^{2+} , while transmission electron microscopy (TEM) imaging was used to visualise the nanoparticle distribution. **Results:** The HepG2 cells have significantly taken up Ag^+ from *C. roseus*-AgNPs with at least six times higher compared to Ag^+ from AgNO_3 . The intracellular Ca^{2+} detected in HepG2 cells for all treatments were significantly higher than the untreated cells, in time-dependent manner. TEM images indicated the endocytosis of *C. roseus*-AgNPs with the presence of endosomes and exocytic vesicles. **Conclusion:** The significant accumulation of intracellular Ag^+ demonstrated the efficiency of the *C. roseus*-AgNPs uptake while the increased Ca^{2+} indicated the early sign of cell injury. The cellular uptake was mainly through endocytosis. These findings are crucial to correlate the physicochemical properties of *C. roseus*-AgNPs with the anticancer mechanisms towards the development of liver cancer therapy.

Malaysian Journal of Medicine and Health Sciences (2023) 19(4):171-177. doi:10.47836/mjmh19.4.26

Keywords: *Catharanthus roseus*-silver nanoparticles; HepG2; cellular uptake; ICP-OES; TEM

Corresponding Author:

Nor Hazwani Ahmad, PhD
Email: norhazwani@usm.my
Tel: +604-5622530

has prompted concern regarding their biological effects, especially on the cellular response to rule out the biosafety issues of AgNPs and provide a theoretical basis to develop a better anticancer therapeutic strategy (4).

INTRODUCTION

Nanotechnology has become prominent in recent years, as it has been widely applied in multidisciplinary fields, such as usage in industrial, medical, and consumer products (1). Recent development in nanotechnology has broadened the possible applications of silver nanoparticles (AgNPs). Due to the essential need to develop environmentally and economically friendly approaches to cancer treatment and diagnostics, biosynthesised AgNPs was considered one of the most promising research orientations for oncotherapy (2). Biogenic synthesis of AgNPs offers more benefits as they are more environmentally friendly, risk-free, readily accessible, and cost-effective (3). The unique features of AgNPs have led to rapid commercialisation, which

AgNPs have been extensively studied as biomedical tools for cellular markers in various applications, particularly in vitro and in vivo imaging (5). The ability to monitor and manage Ag and Ca ions accumulation within a cell can improve diagnostic sensitivity and treatment efficiency for biological and clinical applications (6). The fundamental basis of cellular uptake and interaction requires a few important considerations. Previous studies have shown that AgNPs could easily reach the human body by bypassing natural mechanical barriers and being taken up by the cells due to their nano-scale dimension (7). In general, intravesicular AgNPs localisation is affected by various mechanisms that differ according to their physical and chemical properties, such as phagocytosis, micropinocytosis, receptor-mediated endocytosis, or adhesive interactions (8). A better understanding of

cellular uptake mechanisms would lead to an in-depth perception of AgNPs cytotoxicity toward cancer cells. Therefore, in this study, we investigate the cellular uptake of biosynthesised AgNPs using *Catharanthus roseus* (L.) G. Don by hepatocellular carcinoma cells HepG2 cells by looking at the accumulation of intracellular Ag⁺ and Ca²⁺ intracellular. This is followed by the evaluation of the *C. roseus*-AgNPs distribution in HepG2 cells.

MATERIALS AND METHODS

Plant materials

C. roseus plants were obtained in Teluk Air Tawar, Butterworth, Penang. The plants were submitted to the Herbarium Unit, School of Biological Sciences, and Universiti Sains Malaysia (USM) for identification. The voucher material was deposited at the same herbarium with a reference number 10933 (9).

Synthesis of *C. roseus* aqueous extract

The leaves part of *C. roseus* was used as mentioned in our previous study (9). Briefly, the *C. roseus* plants were collected from the nearby area in Butterworth, Penang. Then, the leaves were separated and washed using double distilled water. This was followed by a drying process until the leaves became completely brittle. The aqueous extraction was performed by mixing 50 g of the ground dried leaves with 1 L of double distilled water and placed in a 40 °C shaker water bath (Mettler, Germany) overnight. The extract was then filtered and centrifuged (Eppendorf, USA) twice at 2000 rpm for 15 minutes. Following the centrifugation, only the supernatant was collected and ready for the freeze-drying process using a freeze dryer (FDU-1200, Eyela, USA). The freeze-dried final product was ready to use for further experiment.

Synthesis of *C. roseus*-AgNPs

The preparation of *C. roseus*-AgNPs was performed according to our previous study (10). Briefly, 10% of *C. roseus* aqueous extract was mixed with 5mM of silver nitrate (AgNO₃) solution, followed by incubation at room temperature. The colour of the mixture was monitored until the colour changed to dark brownish. The pellet was collected after centrifugation at 10,000 rpm for 15 minutes and washed using sterile distilled water several times to obtain clean *C. roseus*-AgNPs. The excessive water was removed by drying the *C. roseus*-AgNPs in the vacuum oven (Thermo Fisher Scientific, USA) at 40 °C.

HepG2 cell line

The HepG2 cell line (liver hepatocellular carcinoma) was purchased from the American Type Culture Collection (ATCC, USA). The culture method was performed as recommended by the cell line manufacturer, using RPMI-1640 complete medium. The complete medium was prepared by mixing RPMI-1640 medium (Nacalai Tesque, Japan), 10% heat-inactivated fetal bovine serum

(Gibco, USA), 1% 100 units/mL penicillin-streptomycin (v/v) (Nacalai Tesque, Japan) and 1% L-glutamine (v/v) (Gibco, USA). The cells were cultured in cell culture flasks and incubated at 37°C in an incubator (Shellab, USA) supplied with 5% CO₂. The growth and proliferation of the cells were monitored until it reached 70-80% confluency for further use.

Quantification of intracellular Ag⁺

Inductively coupled plasma optical emission spectroscopy (ICP-OES) (Perkin Elmer Optima, USA) was used to investigate the uptake of Ag ions into HepG2 cells. The cells were seeded at a concentration of 1x10⁵ cells/mL in six-well tissue culture (BD Biosciences, USA) and incubated overnight. The cells were then exposed to mean IC₅₀ values of *C. roseus*-AgNPs, camptothecin and *C. roseus* aqueous extract which were obtained from our previous study (10); 4.95±0.26 µg/mL, 0.73±0.29 µg/mL, 51.89±0.27 µg/mL, respectively. Treatment with AgNO₃ was performed at a concentration of 5 mM. Untreated HepG2 cells were used as control. Following the incubation, the cells were collected, rinsed with sterile phosphate-buffered saline (PBS) solution, and centrifuged at 6000 rpm for 10 minutes. The collected cells were pre-digested overnight with 9 mL of 70% HNO₃, and the mixture was then irradiated in closed vessels with a microwave digester (Perkin Elmer, USA) for 10 minutes at 120 °C, followed by 180 °C for 30 minutes. After the digestion process, the sample was diluted with 10 mL deionised water and kept at 4 °C for further analysis. The uptake of *C. roseus*-AgNPs was quantified by the ICP-OES and a silver standard solution (1000 mg/l-1 in 5% HNO₃) was used as standard.

Quantification of intracellular Ca²⁺

The Ca²⁺ measurement was done using inductively coupled plasma optical emission spectroscopy (ICP-OES, Perkin Elmer Optima). The cells were seeded at a density of 1x10⁵ cells/mL in six-well plates (BD Biosciences, USA) and incubated overnight. The cells were then treated with mean IC₅₀ values of *C. roseus*-AgNPs (4.95±0.26 µg/mL), camptothecin (0.73±0.29 µg/mL) and *C. roseus*-aqueous extract (51.89±0.27 µg/mL) for 24, 48 and 72 hours, respectively. Treatment with AgNO₃ was performed at a concentration of 5 mM. Untreated HepG2 cells were used as control. Following the incubation, the cells were collected and washed several times with sterile phosphate-buffered saline (PBS) solution. The cells were centrifuged at 6000 rpm for 10 minutes. The cells were digested in closed vessels with a microwave digester (Perkin Elmer, USA).

Visualisation *C. roseus*-AgNPs distribution

The cellular uptake of *C. roseus*-AgNPs to HepG2 cells was visualised using transmission electron microscopy (TEM) Phillips CM12 with Docu Version 3.2 image processing. The cell preparation method was performed according to the manufacturer's standard protocol. The cells were initially prepared at a concentration of 1x10⁵

cells/mL. The treatment was performed using the *C. roseus*-AgNPs IC₅₀ values and incubated for 24, 48, and 72 hours. Following the *C. roseus*-AgNPs exposure, the cells were thoroughly rinsed using PBS and subsequently fixed with McDowell-Trump fixative (VWR, USA) for 72 hours at 4 °C followed by postfix in 1% osmium tetroxide (Sigma Aldrich, USA). The cells were dehydrated for 15 minutes in a graded sequence of ethanol (Merck, USA) concentrations ranging from 50% up to 100%, followed by further dehydration with 100% of acetone (Merck, USA). After the dehydration process, the cells were initially infiltrated with resin-acetone: Spurr's resin mix (1:1) for 2 hours and subsequently embedded with 100% resin at 50 °C overnight. Ultrathin sections (10-20 nm) of the resin embedded cells samples blocks were obtained by trimming process using PowerTomeXL-RMC (Boeckeler Instrument Inc, Arizona) and transferred onto a 3 mm 300 mesh copper grid (SPI supplies, USA). Prior to imaging with the FEI CM12 Transmission Electron Microscope (Phillips, USA), the sections were stained with 2% uranyl acetate (Sigma Aldrich, USA) and 2% lead citrate (Sigma Aldrich, USA).

Briefly, 9 mL of 70% HNO₃ was added, and the mixture was irradiated at 120 °C for 10 minutes, followed by 180 °C for 30 minutes. The sample was diluted with 10 mL deionised water and stored at 4 °C for further analysis. The Ca²⁺ was quantified by ICP-OES and a standard calcium solution (1000mg/l in 5% HNO₃) was used as standard.

Statistical analysis

Each experiment was performed in triplicate. For quantification data analysis, the results were expressed as mean ± standard deviation (SD). A two-way ANOVA with post hoc Dunnett test was used to calculate the significant differences between control and treated samples, while a two-way ANOVA with post hoc Bonferroni was used for multiple comparisons, particularly between *C. roseus*-AgNPs treatment and AgNO₃ treatment.

RESULTS

Quantification of intracellular Ag⁺

The Ag⁺ taken up by HepG2 cells was quantified using ICP-OES, as depicted in Figure 1. The uptake of Ag⁺ by HepG2 after exposed to *C. roseus*-AgNPs was significantly (p < 0.001) higher compared to the untreated cells which were 3.55±0.02 µg/mL, 2.80±0.04 µg/mL and 2.50±0.03 µg/mL at 24, 48, and 72 hours, respectively. In comparison, the concentration of intracellular Ag⁺ in response to AgNO₃ treatment was 0.43±0.004 µg/mL, 0.42±0.004 µg/mL and 0.44±0.0003 µg/mL at 24, 48 and 72 hours, respectively. The Ag⁺ accumulation is also significantly higher compared to the untreated cells. It is important to note that the concentration of Ag⁺ from *C. roseus*-AgNPs treatment was found higher compared to AgNO₃ treatment with at least six times

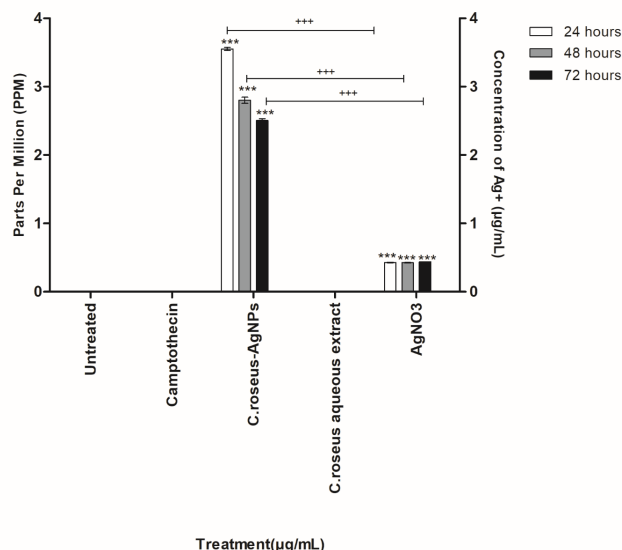


Figure 1: Intracellular Ag⁺ in HepG2 cells using ICP-OES. All experiments were done in triplicate, and the data represent means ± standard deviation. The comparison between each treatment with untreated cells and *C. roseus*-AgNPs treated cells was done using two-way ANOVA with Dunnett's post-test to detect any significant differences (* p < 0.05; ** p < 0.01; *** p < 0.001; ns not significant to untreated cells). Comparison between *C. roseus*-AgNPs and AgNO₃ was done using two-way ANOVA with Bonferroni post-test for multiple comparisons to detect any significant differences (+ p < 0.05; ++ p < 0.01; +++ p < 0.001; ns not significant).

higher. Another observation was the pattern between these two treatments was opposite in time dependent manner, whereby the Ag⁺ concentration was increased for *C. roseus*-AgNPs treatment and decreased for AgNO₃ treatment. This finding is also presented by intensity values, measured in count/second (c/s) unit, as shown in Table I. The quantitative intensity measurement of the Ag⁺ element was performed at the wavelength of 328.068. Cells treated with *C. roseus*-AgNPs showed a significant (p < 0.001) intensity values at 328.068 wavelength with 20318.7 c/s, 15929.6 c/s, and 14197.1 c/s at 24, 48 and 72 hours, respectively. Whereas the intensity values from the AgNO₃ treatment were 41.5 c/s, 40.9 c/s, and 42.6 c/s at 24, 48 and 72 hours, respectively. As predicted, there were no values obtained for the untreated cells and treatment with camptothecin and *C. roseus*-aqueous extract, indicating the absence of Ag⁺ elements. Figure 2 shows the representative intensities peak diagrams for Ag⁺ quantification in HepG2 cells using ICP-OES, upon treatment with *C. roseus*-AgNPs and AgNO₃ after 24 hours incubation, to indicate the comparison.

Table I: The intensity values (count/second) of Ag⁺ in HepG2 cells using ICP-OES at 24, 48 and 72 hours for the untreated and cells treated with camptothecin, *C. roseus*-AgNPs, *C. roseus* aqueous extract and AgNO₃. NA indicates not available due to absence of Ag⁺

Incubation (hours)	Intensity of Ag ⁺ (count/second)				
	Untreated	Camptothecin	<i>C. roseus</i> -AgNPs	<i>C. roseus</i> aqueous extract	AgNO ₃
24	NA	NA	20318.7	NA	41.5
48	NA	NA	15929.6	NA	40.9
72	NA	NA	14197.1	NA	42.6

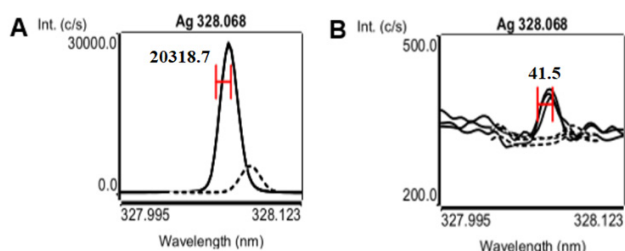


Figure 2: Representative intensities peak diagram for Ag⁺ quantification in HepG2 cells using ICP-OES, upon treatment with A) *C. roseus*-AgNPs and B) AgNO₃ after 24 hours incubation.

Quantification of intracellular Ca²⁺

The amount of intracellular calcium content in the cells is depicted in Figure 3. Noticeably, all treatments have induced significant ($p < 0.001$) Ca²⁺ accumulation in HepG2 cells compared to the untreated HepG2 cells, in time-dependent manner. The concentration of intracellular Ca²⁺ obtained for the untreated cells were 0.13±0.001 µg/mL, 0.14±0.001 µg/mL and 0.14±0.002 µg/mL after 24, 48 and 72 hours incubation, respectively. In comparison, the concentration of Ca²⁺ detected in HepG2 cells treated with *C. roseus*-AgNPs were 0.31±0.003 µg/mL, 0.40±0.005 µg/mL and 0.45±0.014 µg/mL at 24, 48 and 72 hours respectively. Interestingly, a significant ($p < 0.001$) reduction of Ca²⁺ was observed in cells treated with AgNO₃ compared to the cells treated with *C. roseus*-AgNPs. These findings are supported by the results of the Ca²⁺ intensity values (count/second, c/s) as shown in Table II. The values indicate the

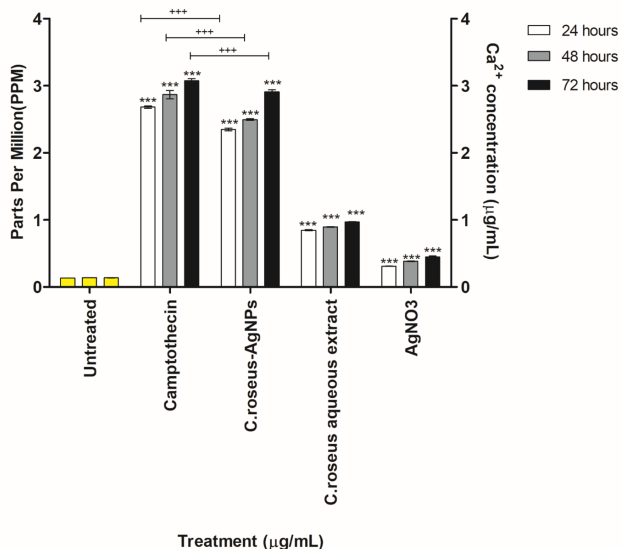


Figure 3: Intracellular Ca²⁺ in HepG2 cells using ICP-OES. All experiments were done in triplicate, and the data represent means ± standard deviation. The comparison between each treatment with untreated cells and *C. roseus*-AgNPs treated cells was done using two-way ANOVA with Dunnett’s post-test to detect any significant differences (* $p < 0.05$; ** $p < 0.01$; *** $p < 0.001$; ns not significant to untreated cells). Comparison between *C. roseus*-AgNPs and AgNO₃ was done using two-way ANOVA with Bonferroni post-test for multiple comparisons to detect any significant differences (+ $p < 0.05$; ++ $p < 0.01$; +++ $p < 0.001$; ns not significant).

Table II: The intensity values (count/second) of Ca²⁺ in HepG2 cells using ICP-OES at 24, 48 and 72 hours for the untreated and cells treated with camptothecin, *C. roseus*-AgNPs, *C. roseus* aqueous extract and AgNO₃. NA indicates not available due to absence of Ag⁺

Incubation (hours)	Intensity of Ag ⁺ (count/second)				
	Untreated	Camptothecin	<i>C. roseus</i> -AgNPs	<i>C. roseus</i> aqueous extract	AgNO ₃
24	1419.7	18476.5	16306.5	7785.5	3321.4
48	1532.5	19689.9	17258.7	8924.2	3874.5
72	1587.4	21022.2	19969.1	10241.5	3968.8

quantitative intensity measurement of Ca²⁺ element at the wavelength of 396.847. The intensity for *C. roseus*-AgNPs treatment were 1630658 c/s, 1725872 c/s, and 1996912 c/s at 24, 48 and 72 hours, respectively. In comparison, upon treatment with AgNO₃, the intensity values were lower with 3321.4 c/s, 3874.5 c/s, and 3968.8 c/s at 24, 48, and 72 hours, respectively. Figure 4 shows the representative intensities peak diagrams for Ca²⁺ quantification in HepG2 cells using ICP-OES, upon treatment with *C. roseus*-AgNPs and AgNO₃ after 24 hours incubation, to indicate the comparison.

Visualisation *C. roseus*-AgNPs uptake

In the TEM electron micrographs, the *C. roseus*-AgNPs appear as dark spots in B-F. As depicted in Figure 5(A), no morphological abnormalities were observed in the untreated HepG2 cells and the cell membrane remain intact. Figure 5(B) clearly shows the initial interaction between *C. roseus*-AgNPs and the cell membrane of HepG2 after 24 hours incubation. Figure 5(C) shows further internalisation of densely packed *C. roseus*-AgNPs agglomerates into the HepG2 cells through the formation of membrane-enclosed structures which likely represents an early endosome. Figure 5(D) shows a homogeneous intracellular distribution of *C. roseus*-AgNPs in the cytoplasm. It can be seen some of the endosomes encapsulate loosely packed nanoparticle (white arrow) and densely packed nanoparticles (black arrow). After 48 hours, more prominent and scattered nanoparticles were detected that resembles the endosome as shown in Figure 5(E). Meanwhile, Figure 3(F) indicates presence of exocytic vesicles at the cell periphery containing *C. roseus*-AgNPs and debris after 72 hours, accompanied with loss of cellular membrane integrity.

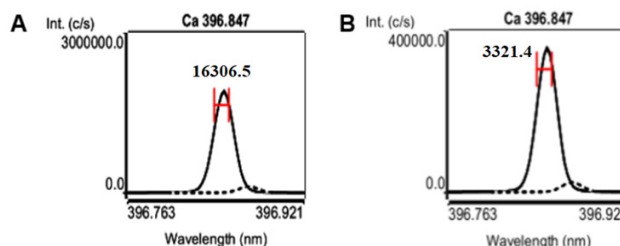


Figure 4: Representative intensities peak diagram for Ca²⁺ quantification in HepG2 cells using ICP-OES, upon treatment with A) *C. roseus*-AgNPs and B) AgNO₃ after 24 hours incubation.

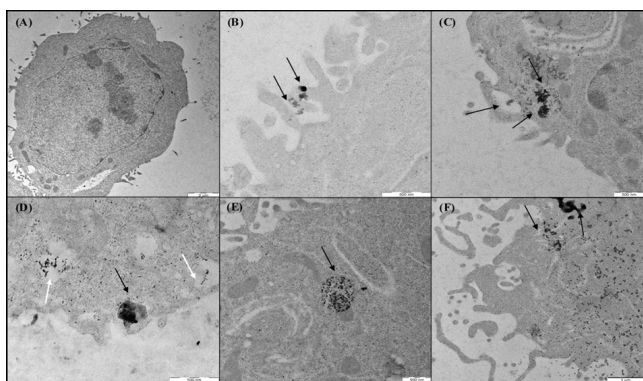


Figure 5: TEM images of HepG2 cells with up taken *C. roseus*-AgNPs. In the TEM images, the nanoparticles appear as dark spots in B-F. There is no AgNPs uptake in the untreated cells (A). After 24 hours, the uptake of the *C. roseus*-AgNPs can be clearly seen at the cell periphery (B). Agglomerates of *C. roseus*-AgNPs encapsulated in early endosome (C). Homogeneous intracellular distribution of *C. roseus*-AgNPs in the cytoplasm, with encapsulated loosely packed nanoparticle (white arrow) and densely packed nanoparticles (black arrow) (D). After 48 hours, prominent loosely arranged nanoparticles in endosome (E). Presence of exocytic vesicle after 72 hours (F).

DISCUSSION

The current updates of the cellular uptake mechanism of AgNPs are limited due to the unresolved issues regarding the intricacy of AgNPs properties (6, 11). Comprehensive approaches are necessary to understand the cellular uptake of AgNPs that would shed light to the mechanisms of toxicity and their potential therapeutic application for cancer treatment. In this study, we investigated the cellular uptake of *C. roseus*-AgNPs by HepG2 cells by quantitative measurement of intracellular Ag^+ and Ca^{2+} using ICP-OES. In addition, the localisation of intracellular *C. roseus*-AgNPs in HepG2 cells were visualised by TEM.

Our findings demonstrated that HepG2 cells have taken up a significant amount of Ag^+ from *C. roseus*-AgNPs in comparison to AgNO_3 especially at 24 hours with almost 3-fold difference of the intracellular Ag^+ concentration. The uptake efficiency of AgNPs is believed to be size-dependent, and it has been suggested that the average particle size between 20 and 50 nm is ideal for optimum cellular uptake efficiency (12). This linking corroborates with our previous study which indicated the average size of the *C. roseus*-AgNPs particle was 30 nm, suggesting that the uptake might occur at an optimum efficiency (13). Additionally, more publications that studied on different types of nanoparticles like AuNPs, iron oxide nanoparticles and AgNPs have concluded that a maximum efficiency of cellular uptake was achieved at particle size in the range between 30 and 50 nm (14). In general, this suggests that nano-sized particles from 20 nm to 50 nm produces better cellular uptake efficiency. The AgNPs can enter cells via endocytosis with four possible mechanisms of entry; macropinocytosis, clathrin-mediated endocytosis, caveolae-mediated endocytosis and clathrin independent and caveolae

independent pathway (12). Hence, further study is necessary to rule out the mechanism of entry of the *C. roseus*-AgNPs that would correlate the physico-chemical properties of AgNPs with the mechanism of entry. Our findings are in line with a study done by Hua Guo et. al that indicated the AgNPs accumulated in the primary human umbilical vein endothelial cells was significantly higher compared to AgNO_3 (15). Moreover, another group of researchers have demonstrated that the concentration of intracellular Ag^+ were increased in time-dependent manner when the human glioblastoma cells U251 were treated with AgNPs (11).

Apart from size, the surface charge of nanoparticles also play a crucial role that influence the cellular uptake efficiency (16, 17). The surface charge of *C. roseus*-AgNPs was previously confirmed in our study, with -16.6 mV that would support the cellular uptake efficiency of Ag^+ obtained in this study (18). Interestingly, previous review paper has summarised that positively charged NPs are mainly internalised by the cell via micropinocytosis whereby negatively charged NPs are taken up through clathrin-/caveolae-independent endocytosis (19). Hence, we speculate that our negatively charged AgNPs have entered the non-phagocytic cells HepG2 cells via clathrin-/caveolae-independent endocytosis, at an optimal cellular uptake efficiency. In fact, several authors suggested that endocytosis is the major pathway of the nanoparticle's uptake by cells while the ionic form of Ag are taken up with the involvement of transport proteins at the cell membrane (20, 21).

Intracellular calcium level is assumed to be one of the screening tools for nanoparticle toxicity (22). Disruption of calcium homeostasis is an indicator of early sign of cell injury, as the calcium ions trigger the activation of catabolic enzymes that responsible for the toxicity effects. Multiple series of calcium influx and efflux particularly in mitochondria would lead to the oxidative stress and eventually initiate the cascade pathway of apoptosis (23). Our study shows that all treatments which were *C. roseus*-AgNPs, camptothecin, *C. roseus* aqueous extract and AgNO_3 have induced significant increment of intracellular Ca^{2+} , in time-dependent manner. Moreover, the highest intracellular Ca^{2+} accumulation in HepG2 cells was observed in response to camptothecin followed by *C. roseus*-AgNPs, *C. roseus* aqueous extract and AgNO_3 . It is important to note that the concentration of Ca^{2+} of camptothecin and *C. roseus*-AgNPs treated cells was between $2.68 \pm 0.02 \mu\text{g/ml}$ and $3.07 \pm 0.03 \mu\text{g/ml}$, compared to the *C. roseus* aqueous extract and AgNO_3 which was below $1 \mu\text{g/ml}$ only. This result demonstrates that both camptothecin and *C. roseus*-AgNPs produced higher cellular toxicity and may provide a strong justification for the anticancer activity. Theoretically, the Ca^{2+} fluctuations is triggered by the Ag^+ release from AgNPs through surface oxidation upon binding to the cell surface receptors (23, 24). Moutin et al. demonstrated that Ag^+ ions operate on the same

location as Ca^{2+} ions and subsequently, the Ag^+ causes Ca^{2+} release from sarcoplasmic reticulum vesicles (25). Hsu et al. reported AgNPs released Ag^+ ions that could lead to cell signaling cascade with calcium homeostasis disruption that are believed to induce cell cycle arrest and inhibit cancer cell division (26, 27).

The AgNPs distribution in HepG2 cells was further evaluated by TEM. As expected, the *C. roseus*-AgNPs were initially penetrated the cells where they are localised at the periphery of the cellular membrane following 24 hours. Some of the *C. roseus*-AgNPs were further internalised through the formation of endosomes while others remain as free nanoparticles in the cytoplasm. Hence, direct uptake without the formation of endosomes could also take place. Furthermore, the nanoparticles were observed in aggregates and loosely arranged especially after 48 hours. Following 72 hours, exocytic vesicles were observed at the cell periphery containing nanoparticles and cellular debris. Our results are in accordance with other studies that demonstrated similar intravesicular particle distribution and pattern (28–30).

CONCLUSION

The present study demonstrated that the *C. roseus*-AgNPs were taken up by non-phagocytic hepatocellular carcinoma cells HepG2 at an optimal efficiency through the significant accumulation of intracellular Ag^+ . The cellular uptake was mainly through endocytosis and suggested that the intracellular Ca^{2+} might contribute to the cytotoxic effects. The pattern of the nanoparticle's distribution throughout the incubation period observed by the TEM has enlightened the process of the uptake. All these parameters have addressed the physicochemical properties of *C. roseus*-AgNPs which correlates with their anticancer activity. These findings suggest that the *C. roseus*-AgNPs have the potential to be considered as newly developing inorganic nanoparticles for liver cancer therapy. However, further detailed studies are necessary to evaluate the cellular uptake's mechanism, including the signaling pathway at the molecular level. More importantly, our study also demands for further investigation in regards with the nanoparticle toxicity on normal cells counterpart.

ACKNOWLEDGEMENTS

We would like to offer special appreciation to all laboratory staffs and postgraduate students under the AMDI centralised laboratory for their guidance, assistance, and support. This study was funded by Fundamental Research Grant Scheme (FRGS), with Reference Code: FRGS/1/2015/SG03/USM/03/1 under the Ministry of Higher Education Malaysia.

REFERENCES

1. Piao MJ, Kang KA, Lee IK, Kim HS, Kim S, Choi JYJ, et al. Silver nanoparticles induce oxidative cell damage in human liver cells through inhibition of reduced glutathione and induction of mitochondria-involved apoptosis. *Toxicol Lett* [Internet]. 2011 Feb 25 [cited 2018 Mar 25];201(1):92–100. doi:10.1016/j.toxlet.2010.12.010
2. Huang Y, He L, Liu W, Fan C, Zheng W, Wong YS, et al. Selective cellular uptake and induction of apoptosis of cancer-targeted selenium nanoparticles. *Biomaterials* [Internet]. 2013;34(29):7106–16. Adoi:10.1016/j.biomaterials.2013.04.067
3. Khorrami S, Zarrabi A, Khaleghi M, Danaei M, Mozafari MR. Selective cytotoxicity of green synthesized silver nanoparticles against the MCF-7 tumor cell line and their enhanced antioxidant and antimicrobial properties. *Int J Nanomedicine* [Internet]. 2018 [cited 2020 Sep 1];13:8013–24. Available from: /pmc/articles/PMC6267361/?report=abstract
4. Fruhlich E. The role of surface charge in cellular uptake and cytotoxicity of medical nanoparticles [Internet]. Vol. 7, *International Journal of Nanomedicine*. Dove Press; 2012 [cited 2019 Feb 20]. p. 5577–91. Available from: <http://www.ncbi.nlm.nih.gov/pubmed/23144561>
5. Kapara A, Brunton V, Graham D, Faulds K. Investigation of cellular uptake mechanism of functionalised gold nanoparticles into breast cancer using SERS. *Chem Sci*. 2020;11(22):5819–29. doi: 10.1039/D0SC01255F
6. Chithrani BD, Chan WCW. Elucidating the mechanism of cellular uptake and removal of protein-coated gold nanoparticles of different sizes and shapes. *Nano Lett* [Internet]. 2007 [cited 2018 May 3];7(6):1542–50. doi:10.1021/nl070363y
7. Loutfy SA, Al-Ansary NA, Abdel-Ghani NT, Hamed AR, Mohamed MB, Craik JD, et al. Anti-proliferative activities of metallic nanoparticles in an in vitro breast cancer model. *Asian Pacific J Cancer Prev*. 2015;16(14):6039–46. doi: 10.7314/apjcp.2015.16.14.6039.
8. Maduraiveeran G, Sasidharan M, Ganesan V. Electrochemical sensor and biosensor platforms based on advanced nanomaterials for biological and biomedical applications. Vol. 103, *Biosensors and Bioelectronics*. Elsevier Ltd; 2018. p. 113–29. doi: 10.1016/j.bios.2017.12.031
9. Ghozali SZ, Ismail MN & Ahmad NH. Characterisation of Silver Nanoparticles using a Standardised *Catharanthus roseus* Aqueous Extract. *Malaysian Journal of Medicine and Health Sciences* 2018;14(SUPP1):120–125
10. Azhar NA, Ghozali SZ, Abu Bakar SA, Lim V, Ahmad

- NH. Suppressing growth, migration, and invasion of human hepatocellular carcinoma HepG2 cells by *Catharanthus roseus*-silver nanoparticles. *Toxicol Vitro*. 2020 Sep 1;67(10):4910. doi: 10.1016/j.tiv.2020.104910.
11. AshaRani P V., Hande MP, Valiyaveetil S. Anti-proliferative activity of silver nanoparticles. *BMC Cell Biol* [Internet]. 2009 Sep 17 [cited 2020 Sep 28];10(1):65. doi:10.1186/1471-2121-10-65
 12. Fruhlich E. The role of surface charge in cellular uptake and cytotoxicity of medical nanoparticles [Internet]. Vol. 7, *International Journal of Nanomedicine*. Dove Press; 2012 [cited 2022 Sep 18]. p. 5577–91. Available from: /pmc/articles/PMC3493258/
 13. Ghozali SZ, Vuanghao L NA. Biosynthesis and Characterization of Silver Nanoparticles using *Catharanthus roseus* Leaf Extract and its Proliferative Effects on Cancer Cell Lines. *J Nanomed Nanotechnol*. 2015;06(04):1–10. doi: 10.4172/2157-7439.1000305
 14. Wu M, Guo H, Liu L, Liu Y, Xie L. Size-dependent cellular uptake and localization profiles of silver nanoparticles. *Int J Nanomedicine* [Internet]. 2019 [cited 2022 Sep 16];14:4247–59. doi: doi: 10.2147/IJN.S201107
 15. Guo H, Zhang J, Boudreau M, Meng J, Yin J jie, Liu J, et al. Intravenous administration of silver nanoparticles causes organ toxicity through intracellular ros-related loss of interendothelial junction. *Part Fibre Toxicol* [Internet]. 2016 Apr 29 [cited 2022 Sep 14];13(1). doi: 10.1186/s12989-016-0133-9.
 16. Verma A, Stellacci F. Effect of Surface Properties on Nanoparticle–Cell Interactions. *Small* [Internet]. 2010 Jan 4 [cited 2022 Sep 13];6(1):12–21. doi:10.1002/smll.200901158
 17. Albanese A, Tang PS, Chan WCW. The Effect of Nanoparticle Size, Shape, and Surface Chemistry on Biological Systems. *Annu Rev Biomed Eng* 2012 [Internet]. 2012 [cited 2022 Sep 16];14:1–16. doi: 10.1146/annurev-bioeng-071811-150124.
 18. Ghozali SZ, Ismail MN, Ahmad NH. Characterisation of Silver Nanoparticles using a Standardised *Catharanthus roseus* Aqueous Extract. *Malaysian J Med Heal Sci*. 2018;14(SUPP1):120–5.
 19. Foroozandeh P, Aziz AA. Insight into Cellular Uptake and Intracellular Trafficking of Nanoparticles [Internet]. Vol. 13, *Nanoscale Research Letters*. Nanoscale Res Lett; 2018 [cited 2022 Sep 18]. doi: doi: 10.1186/s11671-018-2728-6.
 20. Brkić Ahmed L, Milić M, Pongrac IM, Marjanović AM, Mlinarić H, Pavičić I, et al. Impact of surface functionalization on the uptake mechanism and toxicity effects of silver nanoparticles in HepG2 cells. *Food Chem Toxicol*. 2017;107:349–61. doi: 10.1016/j.fct.2017.07.016
 21. Wang Z, Li N, Zhao J, White JC, Qu P, Xing B. CuO nanoparticle interaction with human epithelial cells: Cellular uptake, location, export, and genotoxicity. *Chem Res Toxicol* [Internet]. 2012 Jul 16 [cited 2022 Sep 18];25(7):1512–21. doi: 10.1021/tx3002093
 22. Meindl C, Kueznik T, Busch M, Roblegg E, Fruhlich E. Intracellular calcium levels as screening tool for nanoparticle toxicity. *J Appl Toxicol* [Internet]. 2015 Oct 1 [cited 2022 Sep 18];35(10):1150–9. doi:10.1002/jat.3160
 23. AshaRani P V., Mun GLK, Hande MP, Valiyaveetil S. Cytotoxicity and genotoxicity of silver nanoparticles in human cells. *ACS Nano* [Internet]. 2009 Feb 24 [cited 2022 Sep 11];3(2):279–90. doi: 10.1021/nn800596w.
 24. Chinopoulos C, Adam-Vizi V. Calcium, mitochondria and oxidative stress in neuronal pathology: Novel aspects of an enduring theme [Internet]. Vol. 273, *FEBS Journal*. FEBS J; 2006 [cited 2020 Nov 19]. p. 433–50. doi: 10.1111/j.1742-4658.2005.05103.x.
 25. Moutin MJ, Abramson JJ, Salama G, Dupont Y. Rapid Ag⁺-induced release of Ca²⁺ from sarcoplasmic reticulum vesicles of skeletal muscle: a rapid filtration study. *BBA - Biomembr* [Internet]. 1989 Sep 18 [cited 2022 Sep 11];984(3):289–92. doi: 10.1016/0005-2736(89)90295-2.
 26. Orrenius S, McCabe MJ, Nicotera P. Ca²⁺-dependent mechanisms of cytotoxicity and programmed cell death. *Toxicol Lett* [Internet]. 1992 [cited 2022 Sep 11];64–65(C):357–64. doi: 10.1016/0378-4274(92)90208-2.
 27. Hsu YL, Kuo PL, Cho CY, Ni WC, Tzeng TF, Ng LT, et al. *Antrodia cinnamomea* fruiting bodies extract suppresses the invasive potential of human liver cancer cell line PLC/PRF/5 through inhibition of nuclear factor κB pathway. *Food Chem Toxicol* [Internet]. 2007 Jul 1 [cited 2018 Apr 10];45(7):1249–57. doi: 10.1016/j.fct.2007.01.005
 28. Milić M, Leitinger G, Pavičić I, Avdičević Z, Dobrović S, Goessler W, et al. Cellular uptake and toxicity effects of silver nanoparticles in mammalian kidney cells. *J Appl Toxicol* [Internet]. 2014 Jun [cited 2018 Mar 28];35(6):581–92. doi: 10.1002/jat.3081.
 29. Brandenberger C, Mühlfeld C, Ali Z, Lenz AG, Schmid O, Parak WJ, et al. Quantitative evaluation of cellular uptake and trafficking of plain and polyethylene glycol-coated gold nanoparticles. *Small* [Internet]. 2010 Jul 2 [cited 2020 Oct 28];6(15):1669–78. doi:10.1002/smll.201000528
 30. Gliga AR, Skoglund S, Odnevall Wallinder I, Fadeel B, Karlsson HL. Size-dependent cytotoxicity of silver nanoparticles in human lung cells: The role of cellular uptake, agglomeration and Ag release. *Part Fibre Toxicol* [Internet]. 2014 Feb 17 [cited 2020 Nov 10];11(1):11. doi:10.1186/1743-8977-11-11